Collisions of solitary-wave-like objects in a damped driven ferromagnetic system: The Bloch wall

J. J. Żebrowski
Institute of Physics, Warsaw Technical University, Koszykowa 75, PL00-662 Warszawa, Poland
(Received 9 October 1987; revised manuscript received 10 May 1988)

Collisions of excitations in a Bloch wall in stationary motion are studied by numerical means. It is found that these excitations may be either topological (Bloch lines) or nontopological. The excitations have the properties of solitary waves: Even though the Bloch wall is a damped driven system, upon collision the excitations pass through each other, conserving their identity. The interaction of the solitary-wave-like excitations with a nonmagnetic surface of the material is discussed.

I. INTRODUCTION

In magnetic domain-wall dynamics the motion of the Bloch wall is certainly considered a well-understood phenomenon. In most of the cases studied, the Bloch wall is made to move under the influence of a static drive field which is applied parallel to the direction of the magnetization in one of the domains adjacent to the wall. It is well known[1,2] that a characteristic critical value of the drive exists (the Walker critical field) such that, when fields smaller than the critical are applied to the wall, stationary motion ensues. The Bloch wall then moves with a frozen structure and with a constant velocity. In phase space, stationary motion is described by a fixed point attractor.[3] If the drive field exceeds the critical value, a running oscillatory motion of the wall is obtained[1–4] even though the field is only a constant.

In the basic theory of the dynamics of the Bloch wall[1] it is assumed that, since the Bloch wall is, by definition, infinite along its surface, all points on the surface of the Bloch wall are equivalent. Thus, it is assumed to be enough to write the equations of motion describing only the dynamic behavior of the distribution of magnetization in the direction perpendicular to the wall. In the past, some indications were published stating that such an image of the wall in motion may not be complete. By perturbation theory, Slonczewski showed[2] that wall corrugation may occur at drive fields just above the Walker field. In materials with low uniaxial anisotropy, Magyari[5] discussed the stability of the Bloch wall against bending for a narrow range of drive fields just below the critical value. For Bloch walls residing in materials with a large uniaxial anisotropy, it was recently shown that both the distribution along the wall of the magnetization direction and the shape of the wall surface itself may become very complicated when drive fields larger than the Walker field are applied; a strange attractor is obtained.[3]

The purpose of this paper is to study the behavior of excitations which occur in a Bloch wall moving in a static drive field which is smaller than the Walker critical field, i.e., the excitations of a Bloch wall in stationary motion. Attention is restricted to the case of materials with a large uniaxial anisotropy so that the rather complicated problem of the motion of a three-dimensional distribution of the magnetization in a real Bloch wall may be reduced to the dynamics of a Bloch surface[2]: the wall is then treated as a thin membrane of magnetic moments. It shown that the excitations of the Bloch wall structure have certain properties of solitons, i.e., when they collide they pass through each other conserving their identity. The solitonlike structures may be either topological (Bloch lines) or nontopological. The latter excitations have a relatively short lifetime due to the damping acting in the system.

II. EQUATIONS OF MOTION

The Bloch wall in a bulk uniaxial magnetic material is described by the Lagrangian density:

$$L = -M\dot{\varphi}\sin\theta/\gamma - K\sin^2\theta - A[(\nabla\theta)^2+\sin^2\theta(\nabla\varphi)^2] - 2\pi M^2\sin^2\varphi\sin^2\theta + MH_z\cos\theta + E_D \ ,$$

where $4\pi M$ is the saturation magnetization, K the uniaxial anisotropy energy, A is the exchange constant, H_z is the uniform external magnetic field (the drive field) applied along the anisotropy axis, and E_D is the local magnetostatic energy density due to the tilting of the wall with respect to the orientation of the magnetization in the domains; this term is discussed below. The polar angle coordinate $\theta(z,t)$ describes the direction of the magnetization with respect to the anisotropy axis while the azimuthal angle $\varphi(z,t)$—the direction of the magnetization with respect to the surface of the Bloch wall. The z axis is parallel to the applied field direction.

We note here that in this paper only the local magnetostatic term is retained. In conventional domain-wall dynamics formulated for garnetlike materials such an approximation was fully accepted as leading to reasonable results.[6,7] This may seem to be, at a first glance, a rather controversial point in a study of solitary-wave-like behavior as the excitations of the Bloch wall generated in this study contain magnetostatic charges and so interact with each other. The magnetostatic charges within the wall are of several different origins. In vertical Bloch line dynamics it has been known for some time that the magne-

tostatic charges are due to a magnetostatic dipole layer created by the magnetic moments rotating out of the plane of the wall and also to a divergence created by the rotation of the magnetic moments along the length of the vertical Bloch line.[8] It can be shown[8] that the latter type of magnetic charges play a dominant role. Many of the long-range magnetostatic interactions cancel out and the ones that do not are attractive. Incorporation of the long-range magnetostatic interactions of this type with the material parameters used here into the vertical Bloch line model does not induce any qualitatively new behavior but mainly introduces a small phase shift so that all events seem to happen slightly faster before a collision and slightly slower after it.[9] Since the numerical procedure is then considerably slowed down by the need to integrate over all other points in the wall in order to take into account, at a given grid point, the long-range magnetostatic interactions described in Ref. 8, these interactions are neglected here completely.

If horizontal Bloch lines are generated in the wall an additional magnetostatic term appears which need not be discussed in the theory of vertical Bloch lines. This term is due to the fact that, as the wall surface buckles along the length of the Bloch line, magnetostatic charges are created at the boundary between the two domains. In the Appendix a reasonable approximation is made to include the local magnetostatic energy term due to wall buckling. The local-energy term is the largest of all the magnetostatic energy terms. Since tests show that the effect of this term is negligible and since it is the largest of the magnetostatic energy terms, in the calculations presented below the magnetostatic terms due to wall buckling along the easy axis of the magnetization were not included.

In the limit of large uniaxial anisotropy it is usually assumed[1-4] that the azimuthal angle φ is treated as a constant across the wall. Then, if y is the variable perpendicular to the wall, the magnetization distribution in that direction is fully described by the single polar angle θ:

$$\tan\frac{\theta}{2}=\exp\left[\frac{y-q}{\Delta}\right],$$

where $q=q(z,t)$ is the position of the center of the wall and Δ is the Bloch wall width parameter (in this approximation, a constant equal to $\sqrt{A/K}$). In the next step, the Lagrangian density of the system is integrated in the direction perpendicular to the surface of the wall and the following equations of motion may be found:

$$\dot{q}=\gamma\Delta\left[2\pi M\sin(2\varphi)-\frac{2A}{M}\frac{\partial^2\varphi}{\partial z^2}\right]+\alpha\Delta\dot{\varphi},$$

$$\dot{\varphi}=\gamma\left[H_z+\frac{2A}{M}\frac{\partial^2 q}{\partial z^2}\right]-\alpha\frac{\dot{q}}{\Delta}+\gamma\frac{\partial E_D}{\partial q},$$

where α is the phenomenological Gilbert damping constant which comes into the Euler equations through the Rayleigh dissipation function[10]

$$F=\frac{\Delta M}{2\gamma}(\dot{\theta}^2+\sin^2\theta\dot{\varphi}^2).$$

E_D is the demagnetizing energy density per unit area of the wall due to the buckling of the wall along the easy axis direction (see the Appendix for details). The magnetostatic terms due to the buckling of the wall and the long-range magnetostatic terms due to the distribution of the magnetization along the wall for the material parameters used here have a negligibly weak effect on the phenomena studied here and after a certain number of trials have been neglected in the work presented below.

The equations of motion (3) were solved numerically using a modified vector version of the DuFort-Frankel explicite finite difference scheme.[3,11,12] In numerical calculations a Bloch wall of only a finite size along the easy-axis direction may be considered. The size of the wall was 20 μm in the calculations presented here but periodic-boundary conditions were applied to simulate the bulk material case. Two hundred grid points were used for the calculations in which the period of the boundary conditions was 20 μm and 100 grid points—when that period was 12 μm. The time step was 0.05 ns in all cases. The numerical approach used here allowed us to obtain a long-term behavior of the system (over 3 μs) without any signs of a numerical instability.

For initial conditions we assumed that the Bloch wall is initially flat, i.e., $q(z,0)=0$. For the initial distribution along the wall surface of the azimuthal angle $\varphi(z,0)$ it was either assumed to be constant and zero everywhere or that a narrow pulse (0.4–0.6 μm wide) was superimposed on the otherwise flat distribution. The height of that pulse was $\pi/2$ rad.

The following material parameters were used in the calculations: $A=0.81\times10^{-7}$ erg/cm, $4\pi M=140$ G, $\gamma=1.73\times10^{7}$ 1/s Oe, $\Delta=0.029\times10^{-4}$ cm, and $\alpha=0.156$. The Walker critical field for these material parameters $H_w=\alpha 2\pi M=10.9205\pm0.0005$ Oe and the external drive field H_z was varied from zero to the Walker critical field.

III. RESULTS AND DISCUSSION

When the flat initial conditions were used our calculations for all drive fields smaller than the Walker field always reproduced the results of the Walker model[1] for the case of a large anisotropy. The solutions always converged onto a fixed-point attractor (cf. Ref. 3).

For drive fields exceeding the Walker critical limit the perturbation test of Ref. 3 always caused a transition to chaos. Here the perturbation tests were applied to the wall at drive fields lower than the Walker field. These tests[3] simulated the effect of a point fluctuation in the material parameters colliding with the wall for an extremely short time (0.1 ns). Although the magnitude of the amplitude of the fluctuation was varied in a wide range, it was only obtained that the wall state always converged to the fixed-point attractor of Ref. 3.

A different approach was then used. It was decided to perturb the domain wall in stationary motion by using an (unphysical) initial condition in the form of a narrow pulse in the azimuthal angle $\varphi(z,0)$. Depending on the height of this pulse as well as on its width different solitary-wave-like structures were excited within the structure of the domain wall. Note that the domain wall

was moving under the influence of the static drive field at the time these structures were generated.

It was found that if the drive field applied to the wall was significantly smaller than the Walker critical field, the nontopological solitary waves then generated in the initial stage of the motion of the wall decay rather quickly. Because of this effect a decision was made to use $H_z = 10.92$ as the largest drive ($H_w - 0.0005$ Oe) for which the domain wall still does not exhibit a large sensitivity to initial conditions[3] i.e., it remains in the stationary motion state.

The height of the initial condition pulse was varied up to $\pi/2$ rad. For all magnitudes of the pulse amplitude used, the behavior of the system was essentially as described below. Only the boundaries of the specific types of behavior shifted in parameter space as the height of the initial pulse was changed. Below, only the results of calculations performed for the $\pi/2$ initial pulse are presented.

If the width of the pulse in the initial condition $\varphi(z,0)$ exceeded 0.5 μm, only topological solitary waves (a pair of opposite winding Bloch lines) in the wall structure were generated. This can be seen in Fig. 1(a) for a 0.6-μm-wide initial pulse in a Bloch wall moving in a static drive of 10.92 Oe. The solitary wave generated is topologically stable because, in the Bloch wall, $\varphi = n\pi$ with $n = 0, \pm 1, \pm 2, \pm 3, \ldots$ are minimum energy orientations of the magnetic moment. A small "forerunner" pulse precedes each of the kinks in Fig. 1(a). Note that the drive field rotates the magnetic moments outside the solitary wave by some moderate angle away from the exact static minimum of energy position.

The part of the wall where the topological solitary waves are created lags behind the rest of the wall so that a "well" in the shape of the wall surface [Fig. 1(b)] forms simultaneously with the pair of kinks in the wall structure in Fig. 1(a). In Fig. 1(b) the average of the position of the wall q is subtracted at each point of the wall so that the motion of the wall as a while is not visible.

As the motion of the wall continues the kinks in the wall structure (and the respective kinks in the wall shape) move in opposite directions. Because of the periodic-boundary conditions used in the calculations, the left kink of the pair wraps around and reappears on the right of Fig. 1. This is as if, in an infinitely long wall, there were several points at which pairs of Bloch lines were generated so that, after a certain time of motion of the wall, the kinks belonging to adjacent Bloch line pairs approached each other. The forerunner pulses preceding the kinks in the wall structure are the first to collide and some 40/ns later the kinks themselves collide. During the collision at $t = 100-120$ ns the kinks pass through each other. Because of the peculiar angular set of coordinates used, in Fig. 1(a) the kinks look as if a rotation of the magnetic moment to the opposite chirality has occurred at the point of collision. This, however, is not the case: the magnetic moments at the point of collision rotate by 2π. To see that the collision of the solitary waves results in their passing through each other rather than reflecting off each other, note that in Fig. 1(b) the curvature of the wall shape changes sign during the collision process.

With periodic-boundary conditions in effect the wrap-around–collision–wrap-around sequence of events will continue indefinitely, always with only the single pair of kinks taking part. This is in marked contrast to what occurs at drive fields larger than the Walker field: as discussed in detail in Ref. 3 a slight fluctuation of the drive field at a single point in the wall for an extremely short time causes a state of deterministic chaos with many Bloch lines generated and propagating along the wall structure. The wall shape then is also very complicated and dynamically changing. Note that in Fig. 1 the Bloch wall far away from the topological solitary wave is still in the stationary motion state: both the wall shape and its structure seem relatively unaffected by the passing of the excitation.

A lower bound of the drive field magnitude exists below which, when the topological solitary-wave-like excitations of the wall collide, they do not pass through each other but instead annihilate leaving the wall in a purely stationary motion state with $\varphi(z,t) = \text{const}$. The

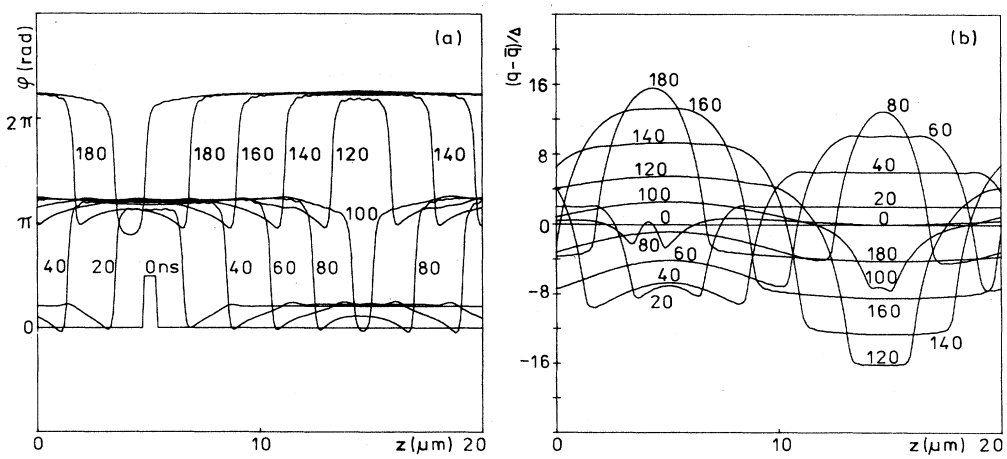

FIG. 1. Collisions of topological solitary waves created by means of a 0.6-μm-wide initial condition pulse in a Bloch wall (periodic-boundary conditions). (a) depicts the wall structure and (b) depicts the shape of the wall surface.

existence of such a lower bound may be easily understood if it is remembered that the system is dissipative. In a nondissipative system the energy in each of the colliding kinks must be conserved so that upon collision they pass through each other regardless of the fact that the system is nonlinear. However, in a dissipative system such as the domain wall, this may not necessarily be true as the energy in the kink-antikink pair may be dissipated during collision. It is only when the power input into the system through the externally applied field exceeds the power dissipated during the collision process that the kinks pass through each other just as solitons do in nondissipative systems. For the material parameters used here the lower bound of the drive field above which the Bloch lines behave as solitary waves was slightly larger than 5 Oe. As noted above all numerical experiments described here were conducted with $H_z = 10.92$ Oe.

If the wall would not reside in an infinite material but in a thick slab of, say 20 μm with force-free boundary conditions assumed at the surfaces of the slab, then the kinks would reflect at these surfaces. This may be seen in Fig. 2 for which the same initial conditions and drive field in Fig. 1 were used; the abrupt rotation of the magnetic moment by 2π at the surface of the slab is accompanied by a change of curvature of the wall shape at that point (not shown). As the right-hand Bloch line of the pair generated from the initial condition pulse moves away to the right, after about 130 ns a secondary pair of topological solitary waves is created behind it. This effect is due to the fact that with force-free boundary conditions the wall shape at the surfaces of the slab, and also inside it, is different than for the periodic-boundary conditions [note here that the cosine magnetostatic potential

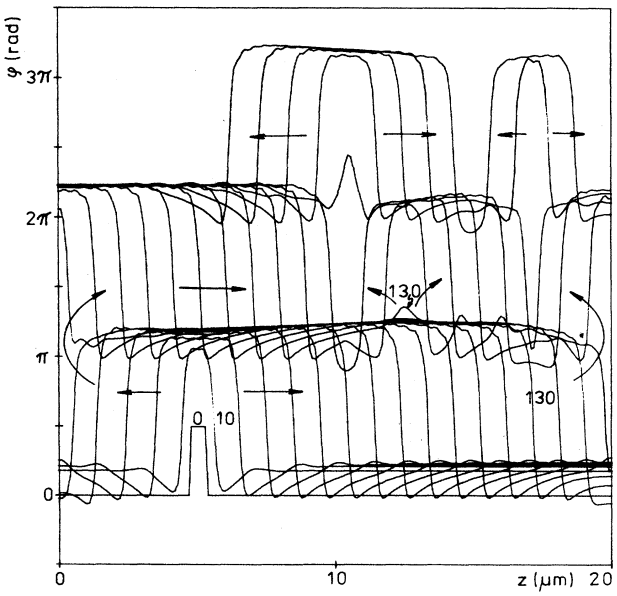

FIG. 2. Collisions of topological solitary waves created by means of a 0.6-μm-wide initial condition pulse in a Bloch wall moving in a slab of a finite thickines—the same as the period in Fig. 1. Unmarked arrows depict direction of motion of the waves.

acts only on the wall structure $\varphi(z,t)$ and not on the wall shape so that, with force-free boundary conditions, the difference in position of the wall at the opposite surfaces of the slab may be very large]. With the drive field magnitude so close to the Walker critical field the large amplitude oscillations of the force-free boundary conditions are able to create an additional pair of solitary-wave-like excitations. Aside from this, the basic behavior of the solitary waves in the thick slab of Fig. 2 is the same as in the case of an infinite wall—they collide and pass through each other while the part of the Bloch far from the excitations remains in stationary motion.

When the width of the initial condition pulse was 0.5 μm or somewhat less, the structure of the wall evolved in a different way than described above. The initial pulse in the wall structure decayed into two nontopological solitary waves in the wall structure moving in opposite directions and preceded by one forerunner pulse each. These pulse solitary waves were each accompanied by a small kink in the shape of the wall. Figure 3 depicts the evolution of the nontopological solitary waves in a domain wall with periodic-boundary conditions during its motion at the Walker critical field. Initially a transient phase occurs during which the solitary waves lose in height and gain in width. However, after about 40 ns of the motion of the wall both these solitary waves transformed into two pairs of topological solitary waves. From then on the behavior of the system was as described before with the solitary waves colliding and passing through each other. No new solitary waves were created after the transition to the topological state.

When the nontopological solitary waves obtained from a 0.4-μm-wide initial condition pulse collide, they pass through each other and the curvature of the wall changes sign, i.e., the solitary waves conserve their identity [Fig. 4(a)—wall structure up to the moment of collision; Fig. 4(b)—after the collision]. However, due to dissipation, the solitary waves which emerge from the collision are very small [note the scale that is two times larger in Fig. 4(b)]. All the same, they decay very slowly so that they may be seen to traverse a certain distance (about 10 μm) within the time limit of the calculation (260 ns) and, in the periodic world of this study, another collision is imminent in Fig. 4.

The role of the forerunner pulses seems significant. When the period of the boundary conditions was decreased to 12 μm so that the collision of the solitary waves could occur earlier, and the rest of the conditions were the same as in Fig. 4, a transition to topological solitary waves was obtained (Fig. 5). The forerunner pulses in this case were still large at the time of collision and close to the solitary waves themselves.

When the nontopological solitary wave obtained from a 0.4-μm-long $\pi/2$ high initial condition pulse in the wall was reflected from the surface of a slab of a 20-μm thickness (force-free boundary conditions), a transition to a topological state of the reflected solitary wave occurred (Fig. 6). During this transition at the surface the other nontopological solitary wave travels to the right without hindrance. However, the reflected topological solitary wave also moves to the right and drives in front of it a

series of small forerunner oscillations which, when they collide with the nontopological solitary wave, destabilize it causing a transition to a pair of topological solitary waves moving in opposite directions. We note here that, when a smaller drive or a smaller initial pulse are used, the nontopological solitary waves may also be simply reflected with a small decrease in size but no transition to topological solitary waves.

In general, the collision time of the nontopological solitary-wave-like excitations is much longer than in the topological case: for the former case it exceeds 60 ns while for the latter it does not exceed 20 ns and was usually in the range of 1–3 ns.

As mentioned above, at drive fields exceeding the Walker field H_w the Bloch wall exhibits a large sensitivity to initial conditions.[3,13] An attempt was made to study the properties of the nontopological solitary-wave-like excitation at the 12 Oe drive field, i.e., H_w+1 Oe. For the first 2 ns the wall structure evolved from the initial condition rectangular pulse as in the other cases described above. At that moment a rapid transition to two pairs of topological solitary waves occurred. The forerunner pulses underwent a similar transition to a pair of topological solitary waves each. As a final state of the wall the strange attractor of Ref. 13 was obtained with a varying number of several topological excitations present in the wall at a given time.

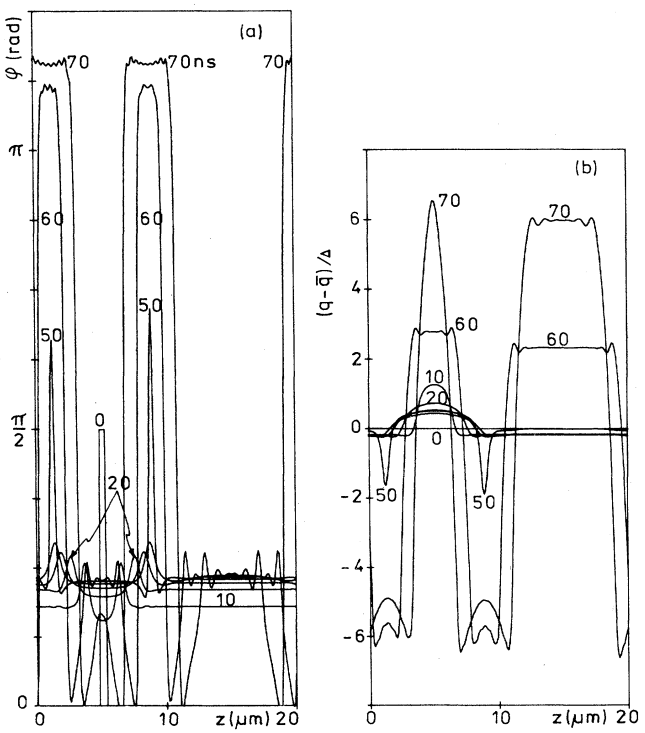

FIG. 3. Spontaneous transition of the nontopological solitary waves created by means of a 0.5-μm-wide initial pulse to pairs of topological waves.

IV. SUMMARY AND CONCLUSIONS

A numerical study of the excitations which may occur during the stationary motion of a Bloch wall in uniaxial ferromagnetic material has been performed. It was confirmed that, for drive fields not exceeding the Walker critical field, the Bloch wall does not have a large sensitivity to initial conditions (cf. Ref. 3). However, the choice of an appropriate form of the initial condition led to the generation of topological or nontopological solitary-wave-like excitations of the Bloch wall moving in a drive field lower than the Walker critical drive. These excitations seem to be well localized in the sense that, far away from them, the wall is seen to be in a stationary motion state which may be somewhat different from the state of an unexcited wall is similar conditions.

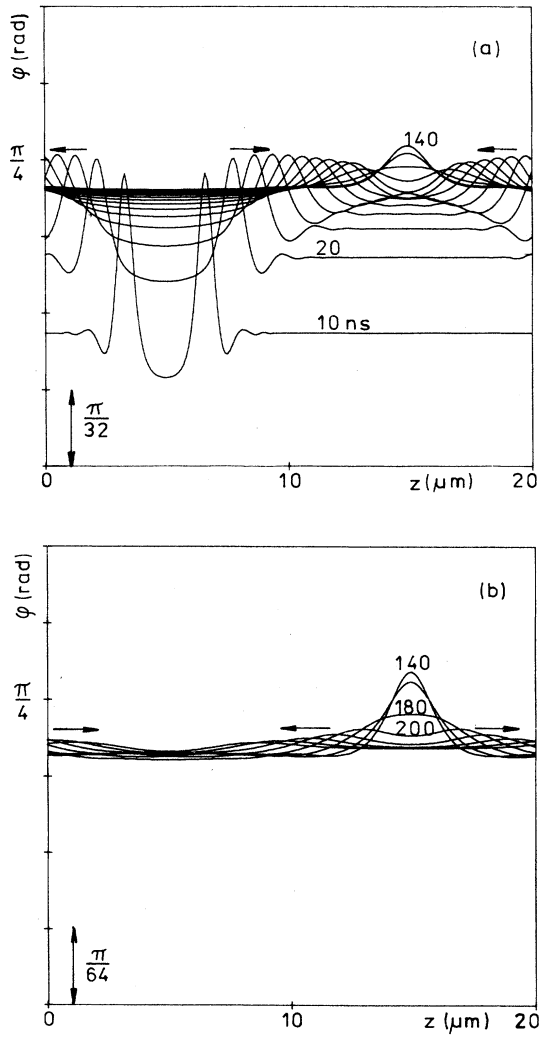

FIG. 4. Collision of nontopological solitary waves created by means of 0.4-μm pulse in a Bloch wall with a 20-μm period. (a) depicts the evolution of the system up to the moment of collision and (b) depicts after the collision. Note the twice larger scale in part b. Unmarked arrows depict direction of motion of the waves.

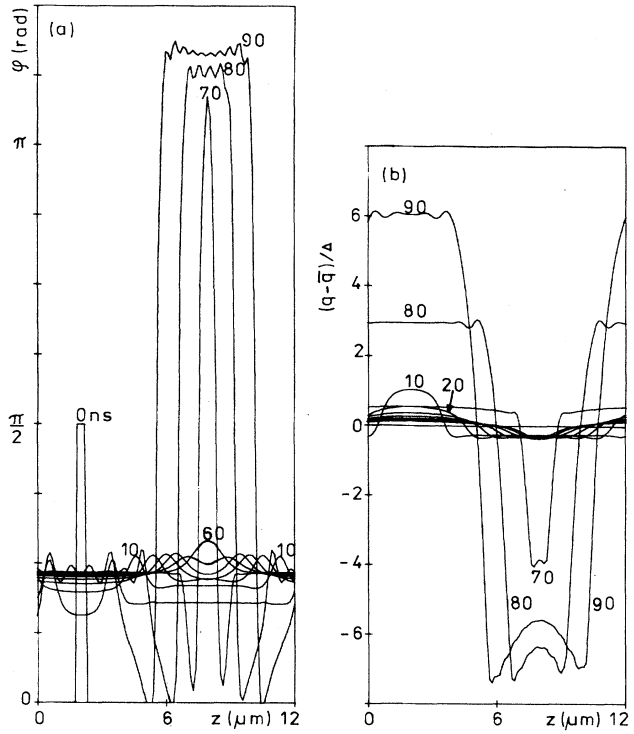

FIG. 5. Instability of the colliding nontopological solitary waves due to a shorter period of the boundary conditions (12 μm). The rest of the conditions as in Fig. 4.

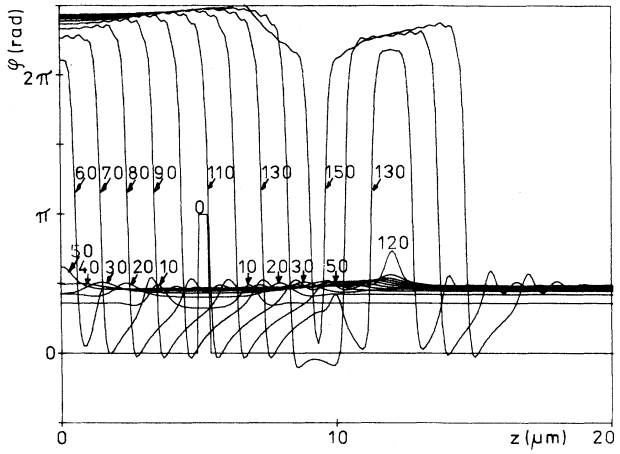

FIG. 6. Instability of the nontopological solitary wave due to its collision with the left surface of the slab at $t=40$ ns. At $t=110$ ns the resultant reflected topological solitary wave causes an instability of the right-hand nontopological wave when the forerunner preceding the reflected topological wave overtakes the former.

The topological solitary-wave-like objects generated in the wall in the course of this study have all the properties of solitons, i.e., they do not disperse nor decay and upon collision they pass through each other conserving their identity. However, the soliton properties are obtained in the dissipative system studied here only if care is taken to provide a large enough power input onto the system so that the energy of the kinks is not dissipated during collision. This may be done by supplying a large enough drive field. Note that in domain-wall dynamics (cf. Refs. 1–4) the possibility of the generation of solitary waves (Bloch lines) below the Walker critical limit has not been acknowledged until now.

The nontopological solitary-wave-like excitations, likewise, seem to have soliton properties. However, the forerunner pulses which precede them do not. As a result, when the solitary-wave-like objects collide two events occur: the height of the pulses decreases abruptly during the collision of the forerunners (these do not reappear after the collision) and, the pulses themselves emerge from the collision considerably broader and much smaller in height. They do conserve their identity during the collision. The fact that the collision time of nontopological solitary waves is so different from that of topological solitary waves probably means that the coupling between the nontopological excitation and the external field is less than in the case of topological solitary-wave-like objects. Note that the pulse solitary waves superimpose on each other rather quickly while the rest of the collision time is taken by the change of sign of the wall surface curvature.

The nontopological solitary wave, generated by means of the rectangular initial pulse condition, at the beginning goes through a transient phase during which it is unstable. This can be seen from the fact that transitions to topological solitary wave excitations occur if the nontopological solitary wave is made to collide either with the surface of the material or with its double. On the other hand, once the wave has had enough time to evolve no such transitions occur and solitonlike properties are observed. However, a collision of the nontopological wave with the topological one results in a transition of the former to a pair of topological waves. The fact that, under certain conditions, a nontopological wave may transform into a pair of topological waves may be understood as an indication that the nontopological wave is a bound state of two kinks.

Finally, note that the phenomena discussed here are different from the instability against bending of the wall discussed in Ref. 5 and corrugated wall motion of Ref. 2, as not only the anisotropy in our case is assumed to be large (the opposite was true in Ref. 5) but also to obtain our results one need not restrict the magnitude of the drive to a value close to the Walker critical field—in the course of this study various excitations were obtained for fields as low as 2 Oe, i.e., about 20% of the Walker field.

ACKNOWLEDGMENTS

The author wishes to thank Professor A. Sukiennicki for many stimulating discussions (Ref. 13) and for an initiation into the exciting field of solitons and nonlinear phenomena. Professor V. I. Nikitenko is warmly thanked for his experimental data on some nontopological solitary-wave-like structures in the domain wall in YIG. Although concerning a material of importantly

different magnetic properties than assumed above, the discussions with Professor V. I. Nikitenko had a strong bearing on the undertaking of this study. Financial support by the University of Lódź under Contract No. CPBP 01.08.B1.1 is gratefully acknowledged.

APPENDIX

To take into account the magnetostatic energy due to buckling of the wall the following may be done. First, note that the local magnetostatic term is always the dominant term. To calculate that term it was assumed that the distribution of magnetostatic charges may be approximated by

$$\sigma=\frac{\partial M}{\partial s}=M^* A \sin^2(\pi s/\Delta) ,$$

where $M^*=M\cos\eta$ with η the angle between the wall and the direction of motion, s is a local variable, the axis of which is normal to the wall. σ was normalized so that the total charge in the wall was $2M^*$ which gave $A=4/\Delta$. The above choice of distribution of magnetostatic charge density was assumed to be convenient and not too distant from the charge distribution obtained in more elaborate models of the head-on domain wall (cf. Ref. 14). Next, σ was integrated over the width of the wall to give

$$M(s)=M^*\frac{2}{\Delta}\left[s-\sin\left[\frac{2\pi s}{\Delta}\right]-\frac{\Delta}{2}\right]$$

and the magnetostatic energy density per unit volume was calculated as $e_D=-\frac{1}{2}H_D M(s)$, where H_D is the demagnetizing field from an infinite planar slab of the thickness Δ and with the magnetization distribution $M(s)$ inside it,

$$H_D=\tfrac{1}{2}\int_0^s\sigma(s')ds'-\tfrac{1}{2}\int_s^\Delta\sigma(s')ds'$$

$$=M^*\frac{2}{\Delta}\left[s-\sin\left[\frac{2\pi s}{\Delta}\right]-\frac{\Delta}{2}\right] ,$$

where the minus sign in front of one integral is due to the opposite directions of the magnetic field contributions from the two parts the wall is divided into by point s. The local magnetostatic energy density per unit area of the wall due to the tilting of the wall was calculated as

$$E_D=-\tfrac{1}{2}\int_0^\Delta H_D M(s)ds=\frac{2m^{*2}}{3}\Delta$$

so that the term to be used in the equations of motion becomes

$$\frac{\partial E_D}{\partial q}=\frac{2M^2}{3}\Delta\sin(2\eta)\frac{\partial\eta}{\partial q} .$$

The calculations presented in this paper were performed with and without the local magnetostatic term included. No difference in the behavior of the solitary waves was observed whether or not the local magnetostatic energy was included in the calculations. Since the local energy term is the dominant one no further attempt was made to include in the equations of motion the other magnetostatic energy contributions.

[1]N. L. Schryer and R. L. Walker, J. Appl. Phys. **45**, 5406 (1974).
[2]J. C. Slonczewski, Int. J. Magn. **2**, 85 (1972).
[3]J. J. Żebrowski and A. Sukiennicki, in Proceedings of the Third International Conference on Physics of Magnetic Materials, Szczyrk, 1986 [Acta Phys. Pol. **A72**, 299 (1987)].
[4]J. Holyst, A. Sukiennicki, and J. J. Żebrowski, Phys. Rev. B **33**, 3492 (1986).
[5]E. Magyari and H. Thomas, Z. Phys. B **59**, 167 (1985).
[6]A. P. Malozemoff and J. C. Slonczewski, *Magnetic Domain Walls* (American, New York, 1979).
[7]J. J. Żebrowski, J. Appl. Phys. **56**, 249 (1984).
[8]R. A. Kosinski and J. Strzeszewski, Phys. Status Solidi B **133**, 533 (1986).
[9]R. A. Kosinski, A. Sukiennicki, and J. J. Żebrowski, J. Phys. (Paris) (to be published).
[10]W. F. Brown, Jr., *Micromagnetics* (Wiley, New York, 1963).
[11]E. Fujita, H. Kawahara, S. Sakata, and S. Konishi, IEEE Trans. Magn. Magn. **20**, 1144 (1984).
[12]B. Carnahan, H. A. Luther, and J. O. Wilkes, *Applied Numerical Methods* (Wiley, New York, 1969).
[13]An early version of this paper was published by J. J. Żebrowski and A. Sukiennicki, in Magnetic Excitations and Fluctuations II, Torino, 1987 [Springer, Proc. Phys. **23**, 130 (1987)].
[14]K. Kaczer, J. Phys. Rad. **20**, 120 (1959).